Monthly Notices
of the
ROYAL ASTRONOMICAL SOCIETY

Mon. Not. R. Astron. Soc. **401,** 1636–1643 (2010) doi:10.1111/j.1365-2966.2009.15799.x

Effects of X-ray irradiation and disc flaring on the [Ne II] 12.8 μm emission from young stellar objects

E. Schisano,[1,2]★ B. Ercolano[3,4] and M. Güdel[5]

[1]*Università degli Studi di Napoli "Federico II",Corso Umberto I, I-80138 (NA), Italy*
[2]*INAF - Osservatorio Astronomico di Capodimonte, Via Moiariello 16, I-80131 Napoli, Italy*
[3]*Institute of Astronomy, Madingley Road, Cambridge CB3 0HA*
[4]*Department of Physics and Astronomy, University College London WC1E 6BT*
[5]*Institute of Astronomy, ETH Zurich, 8093 Zurich, Switzerland*

Accepted 2009 September 28. Received 2009 September 4; in original form 2009 June 5

ABSTRACT

The [Ne II] fine-structure emission line at 12.8 μm has been detected in several young stellar objects spectra. This line is thought to be produced by X-ray irradiation of the warm protoplanetary disc atmospheres; however, the observational correlation between [Ne II] luminosities and measured X-ray luminosities shows a large scatter. Such spread limits the utility of this line as a probe of the gaseous phase of discs, as several authors have suggested pollution by outflows as a probable cause of the observed scatter. In this work, we explore the possibility that the large variations in the observed [Ne II] luminosity may be caused instead by different star–disc parameters. In particular we study the effects that the hardness of the irradiating source and the structure (flaring) of the disc have on the luminosity and spectral profile of the [Ne II] 12.8 μm line. We find that varying these parameters can indeed cause up to an order of magnitude variation in the emission luminosities which may explain the scatter observed, although our models predict somewhat smaller luminosities than those recently reported by other authors who observed the line with the *Spitzer Space Telescope*. Our models also show that the hardness of the spectrum has only a limited (undetectable) effect on the line profiles, while changes in the flaring power of the disc significantly affect the size of the [Ne II] emission region and, as a consequence, its line profile. In particular, we suggest that broad-line profiles centred on the stellar radial velocity may be indicative of flat discs seen at large inclination angles.

Key words: line: formation – line: profiles – planetary systems: protoplanetary discs – stars: pre-main-sequence – infrared: stars – X-rays: stars.

1 INTRODUCTION

Young solar mass stars are surrounded by $\sim 10^{-2}\,M_{\odot}$ of dust and gas distributed in a circumstellar disc which is the birthplace of planetary systems. In recent years, efforts have been made to study the inner regions ($\lesssim$10 au) of these discs in order to constrain gaseous planetary system theories and to understand the physical processes that characterize the warm and chemically active regions of protoplanetary disc atmospheres. Accurate theoretical modelling of the spectral energy distribution (SED) of young stars (see reviews by Dullemond et al. 2007; Natta et al. 2007) coupled with observations in the near and mid-infrared carried out with the *Spitzer Space Telescope* has greatly improved our understanding of the dust component in the inner discs. On the other hand, direct studies of the gaseous component of these discs are more challenging, even though the gas exceeds the dust by over two orders of magnitude in mass. So far molecular line emission, like the CO fundamental and overtones (Najita et al. 2007), the rovibrational transition of water (Carr & Najita 2008; Salyk et al. 2008) and H_2 (Herczeg et al. 2002) have been used as diagnostics of regions with temperatures around 1000–2000 K.

The [Ne II] 12.8 μm line (from now on [Ne II]) has been suggested as a new probe of gas in the potentially planet-forming regions of the inner discs (e.g. Glassgold, Najita & Igea 2007; Hollenbach & Gorti 2009). The ionized region of the disc where this line is formed is heated mainly by X-rays from the central star (Glassgold et al. 2007; Ercolano et al. 2008a; Meijerink, Glassgold & Najita 2008; Glassgold et al., in preparation; but also see Gorti & Hollenback 2008). Indeed, observations from space, with the *Spitzer* Infrared Spectrometer (Espaillat et al. 2007; Lahuis et al. 2007; Pascucci et al. 2007), and from the ground, with Michelle and the Texas Echelon Cross Echelle Spectrograph (TEXES) at Gemini North (Herczeg et al. 2007; Najita et al. 2009) and the VLT imager and Spectrometer for mid-infrared (VISIR) at VLT (van Boekel et al.

★E-mail: schisano@na.astro.it

2009), have successfully detected the [Ne II] line in tens of young systems. The mean observed line luminosity is comparable to the predicted value from disc models, but the scatter of the observed values around this mean spans over three orders of magnitude (e.g. Güdel et al., in preparation). If the [Ne II] line is to be used as a useful diagnostic of the gaseous phase of the inner discs, its origins must be well understood. In particular if the line is formed in the disc by irradiation of the gas by X-rays from the central star then one naturally expects to find a correlation between line luminosity and X-ray luminosity for the observed sources. Such correlation is indeed observed (Pascucci et al. 2007; Güdel et al., in preparation), however, for objects with the same X-ray luminosity the [Ne II] line luminosities span over at least one order of magnitude even after removing those sources with known outflows, for which it can be argued that a large contribution to the line comes from the outflow itself (e.g. T Tau; van Boekel et al. 2009). Understanding the origin of this scatter is extremely important if useful information is to be extracted from future observations of this line. For example, one should expect that disc structural properties, like presence of holes or different degree of flaring, not considered in earlier models have an effect on the [Ne II] emitting region. Moreover, one relevant question is whether the [Ne II] line originates in the bound layers of the disc irradiated mainly by X-rays or whether it includes a contribution from a photoevaporative outflow (e.g. Alexander 2008). In this paper, we will attempt to answer the latter question by exploring the possibility that the scatter observed in [Ne II] line luminosities for a given X-ray luminosity may be due to details of the irradiating field or to the disc structure (i.e. degree of flaring). We will also produce theoretical line profiles and will compare them to available high-resolution observations (e.g. Herczeg et al. 2007; Najita et al. 2009).

We use the models of Ercolano, Clarke & Drake (2009) to calculate [Ne II] line luminosities and line profiles for irradiating spectra of varying hardness. We also show the results from additional models that were run to investigate the effects of disc flaring on the line luminosities and profiles. The paper is organized as follows. The modelling strategy is outlined in Section 2, Section 3 contains a review of our results, while our final conclusions and discussion are given in Section 4.

2 MODELLING STRATEGY AND METHODS

We investigate the effects of two parameters on the [Ne II] emission region of protoplanetary discs: (i) hardness of the irradiating spectrum; (ii) flaring of the disc.

2.1 Hardness of the irradiating spectrum

We calculated fine-structure [Ne II] line luminosities using the temperature and ionization structure obtained by Ercolano et al. (2009) with the MOCASSIN code for EUV+X-ray irradiated protoplanetary discs. We refer to Ercolano et al. (2008a, 2009) for details of the disc models and to Ercolano et al. (2003), Ercolano, Barlow & Storey (2005) and Ercolano et al. (2008b) for details of the code used. The atomic data base included opacity data from Verner et al. (1993) and Verner & Yakovlev (1995), energy levels, collision strengths and transition probabilities from Version 5.2 of the CHIANTI data base (Landi & Phillips 2006, and references therein) and the improved hydrogen and helium free-bound continuous emission data of Ercolano & Storey (2006). In particular the Ne^+ atomic data include collisional strengths of Saraph & Tully (1994) and the transition probabilities of Blackford & Hibbert (1994). We briefly summarize here the model input parameters: we used a stellar mass of 0.7 $M_\odot$, radius 2.5 $R_\odot$, effective temperature of 4000 K and a disc model (d'Alessio 1998) of initial mass 0.027 $M_\odot$ with an outer radius of ∼500 au.[1] The MOCASSIN models are coupled to a hydrostatic equilibrium routine which ensures that the effects of irradiation on the disc structure are taken into account self-consistently (Alexander, Clarke & Pringle 2004; Ercolano et al. 2009). Line luminosities computed without such routine result to be underestimated at worst by a factor of ∼2. The models were irradiated with synthetic spectra extending from the EUV to the X-ray spectral region (13.6 eV–10 keV) where the spectra were calculated using the multitemperature plasma prescription described by Ercolano et al. (2009) and were computed using the PINTOFALE IDL software suite (Kashyap & Drake 2000), adopting the solar chemical composition (Grevesse & Sauval 1998), the atomic data from the CHIANTI compilation (Landi et al. 2006) and ion populations from Mazzotta et al. (1998). The transmittance of the synthetic spectra through neutral screens of varying thickness (as expected to be found in the circumstellar environment of pre-main-sequence stars; e.g. Güdel et al. 2007, 2008) was calculated assuming neutral hydrogen column densities in the range $N_H = 10^{18}$–10^{22} cm^{-2}, with increasing columns resulting in increasingly harder spectra, as the soft radiation is absorbed out. We present [Ne II] luminosities and line profiles for the Ercolano et al. (2009) models labelled in their work as FS0H2Lx1, FS18H2Lx1, FS19H2Lx1, FS20H2Lx1, FS21H2Lx1 and FS22H2Lx1, which consist of models irradiated by spectra screened by columns of 0, 10^{18}, 10^{19}, 10^{20}, 10^{21} and 10^{22} cm^{-2}, and an X-ray luminosity after the screen of L_X (0.1–10 keV) = 2×10^{30} erg s^{-1} ['base luminosity' hereafter; please refer to table 1 in Ercolano et al. (2009) for a full description of the model parameters]. Keeping L_X(0.1–10 keV) constant *after the screen* by normalization of the *absorbed spectrum* was done here in order to isolate the effects of the incoming radiation field hardness alone. Our prescription results in the unscreened models to have a total ionizing luminosity L_{tot}(13.6 eV–10 keV) of approximately twice the X-ray luminosity and the moderately screened models ($N_H = 10^{18}$ cm^{-2}) to have a total ionizing luminosity 1.2 times the base luminosity. We ran four additional models with screens of 0 and 10^{21} cm^{-2} and X-ray luminosities an order of magnitude higher and lower than the base luminosity in order to ensure that any scatter produced by varying screen thickness at fixed $L_X = 2 \times 10^{30}$ erg s^{-1} would also be reproduced for higher or lower X-ray luminosities.

2.2 Disc flaring

In order to investigate the effect of disc flaring on [Ne II] line luminosities, we used a simple analytical description of the disc structure, as given by Robitaille et al. (2006). The density distribution is described by a fixed power-law decline of the surface density in the radial direction coupled with a Gaussian relationship along the z-direction:

$$\rho(R, z) = \rho_0 \left(1 - \sqrt{\frac{R_\star}{R}}\right) \left(\frac{R_\star}{R}\right)^\alpha \exp\left[-\frac{z^2}{2h^2(R)}\right], \quad (1)$$

where ρ_0 is a scalefactor fixed by the disc total mass and $h(R)$ is the disc pressure scaleheight parametrized by a power-law:

$$h(R) = h_{in} \left(\frac{R}{R_{in}}\right)^\beta, \quad (2)$$

where R_{in} and h_{in} are, respectively, the dust destruction radius and the hydrostatic equilibrium scaleheight at this radius. Different

[1] Note that only the inner 50 au of the disc are considered here.

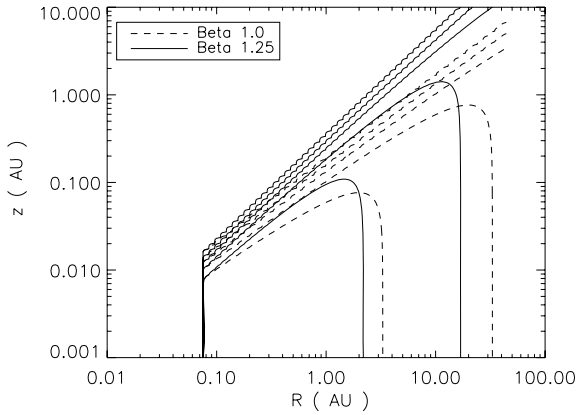

Figure 1. Isodensity curves of the two input disc models used in this work to explore the impact that different degree of flaring has on [Ne II] line luminosity. The black dashed lines show the 'flat' model ($\beta = 1.0$) and solid lines show the 'flared' model ($\beta = 1.25$). The plotted contours refer to increasing densities from 10^5, at higher heights, to 10^{13} g cm^{-3} deeper into the disc with steps of 10^2 cm^{-3}.

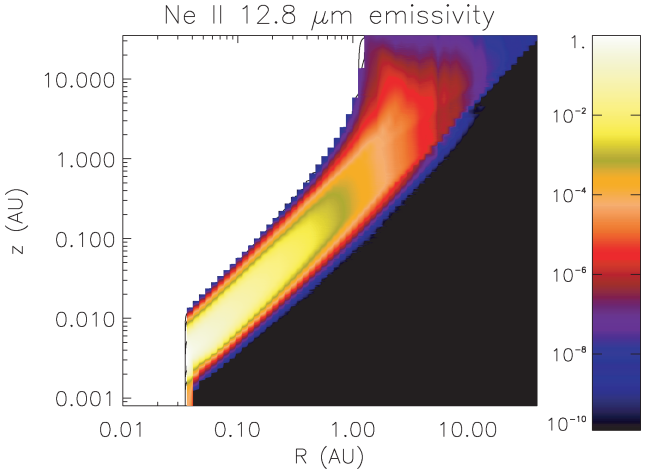

Figure 2. Two-dimensional distribution of the [Ne II] emissivity in arbitrary units for a hydrostatic equilibrium disc model irradiated by an unscreened spectrum.

values of β produce disc models with different degree of flaring, with higher β producing higher flaring. We adopted $\beta = 1.0$ and 1.25 to build models for a 'flat' and 'flared' disc, respectively, and we calculated the corresponding [Ne II] luminosities and line profiles. Such values are also used as limits for the β parameter in the set of SEDs of Robitaille et al. (2006), typically used in the literature to fit real observations. For either density structure we also chose $R_{\rm in}$ corresponding to a dust sublimation temperature of 1600 K, i.e. $R_{\rm in} \sim 0.08$ au with the previous central star parameters, from model comparison with the disc structure of Ercolano et al. (2009) and $\alpha = \beta + 1$ (Whitney et al. 2003a,b) to preserve the surface density distribution power-law scaling $\Sigma(R) \sim R^{-1.5}$ of the minimum solar nebula model of Hayashi (1981; see also Kuchner 2004). The other stellar and disc parameters were chosen to be the same as those used by the Ercolano et al. (2009) models described above. Fig. 1 shows the isodensity curves of the two disc models with different flaring powers. The flat model has a scaleheight reduced typically by a factor of about 3–4 between cylindrical radii from 1 to 10 au when compared to the flared model. In order to isolate the effects of disc flaring only we keep the density structures fixed and do not impose hydrostatic equilibrium on these models.

2.3 Line profiles

We computed line profiles from all our models assuming Keplerian rotation at several disc inclinations. The profiles were computed by summing up the contributions from each cell which produces a Doppler broadened profile given by

$$\Phi(R, \theta, z, v) = \frac{I(R, z)}{\sqrt{2\pi} v_{\rm th}(R, z)} \exp\left\{-\frac{[v - v_{\rm los}(R, \theta)]^2}{2 v_{\rm th}(R, z)^2}\right\}, \quad (3)$$

where $I(R, z)$ is the power emitted by each cell and $v_{\rm th}$ is the local thermal velocity of the Ne^+ ions equal to

$$v_{\rm th}(R, z) = \sqrt{\frac{3 k_B T(R, z)}{m_{\rm Ne} m_{\rm H}}}, \quad (4)$$

and $v_{\rm los}(R, \theta)$ is the cell velocity projected along the line of sight. Given the temperature structure of the disc, the width of the thermal broadening in each cell is $\leq$6 km s^{-1}. We assumed that the mid-plane is optically opaque to the [Ne II] line radiation so only contributions from one side of the disc are taken into account when computing the profile. In fact, adopting the dust cross-section from Weingartner & Draine (2001) of $R_V = 5.5$ extinction law, generally used to reproduce the interstellar extinction in molecular clouds, $\sigma_{12.8\,\mu{\rm m}} = 1.6 \times 10^{-23}$ cm^2/H and $\sigma_{15.5\,\mu{\rm m}} = 1.4 \times 10^{-23}$ cm^2/H, we find that optical depths of the order of 1 are reached for hydrogen column density of about 6–7 $\times 10^{22}$ cm^{-2}. Such column density are reached, for all inclination $\leq$60, at heights of $\leq$0.1 au at a radial distance of 1 and $\sim$1 au at a distance of 10 au, deeper in the disc than the Ne emitting region shown in Fig. 2. In the case of almost edge-on systems, the column density along the line of sight could be large enough to attenuate the observed line intensities, this is not taken into account in this work, but should be in future comparisons with real observations. Finally, we ignore scattered light contribution to the profile, which is negligible in the Weingartner & Draine (2001) dust model that has an albedo of the order of 0.01 at 12.8 μm, but could be significant for different dust models. The resolution of the line profiles we computed is $\lambda/\Delta\lambda \sim 150\,000$, since we summed all together the emission from cells whose $v_{\rm los}$ falls in bins wide 2 km s^{-1}. Moreover, we have convolved the line profiles with a Gaussian function with full width at half-maximum (FWHM) of 10 km s^{-1} to degrade them to a resolution $\lambda/\Delta\lambda \sim 30\,000$, comparable with the high-resolution spectroscopic observations.

3 RESULTS

In this section, we present the line luminosities and profiles obtained from the models described above. Monte Carlo errors on the given line luminosities were obtained by comparing multiple runs of the same model and are about 5 per cent for the lines in question. As in Section 2.3, we will consider the [Ne II] line luminosity response to (i) changes in the shape of the irradiating spectrum and (ii) changes in the disc-density distribution (flaring).

3.1 Hardness of the irradiating spectrum

Table 1 shows the values of [Ne II] 12.8 μm and [Ne III] 15.5 μm line luminosities for models irradiated by the multitemperature thermal spectrum of Ercolano et al. (2009) screened by columns of circumstellar material of thickness 0, 10^{18}, 10^{19}, 10^{20}, 10^{21} and 10^{22} cm^{-2}, respectively (see their fig. 2).

Table 1. [Ne II] and [Ne III] luminosities of disc irradiated by different high-energetic spectrum of $L_X(0.1\text{–}10\,\mathrm{keV}) = 2 \times 10^{30}$ erg s^{-1}.

Model	L_{tot}(13.6 eV–10 keV) (10^{30} erg s^{-1})	[Ne II] (10^{28} erg s^{-1})	[Ne III] (10^{28} erg s^{-1})
Unscreened	4.0	2.3	4.9×10^{-1}
Log $N_h = 18$	2.3	1.9	4.3×10^{-1}
Log $N_h = 19$	2.04	1.7	3.2×10^{-1}
Log $N_h = 20$	2.0	1.5	2.2×10^{-1}
Log $N_h = 21$	2.0	9.1×10^{-1}	1.5×10^{-1}
Log $N_h = 22$	2.0	1.4×10^{-1}	2.5×10^{-2}

Note. The disc model adopted is a d'Alessio disc model, see also Ercolano et al. (2009) for details.

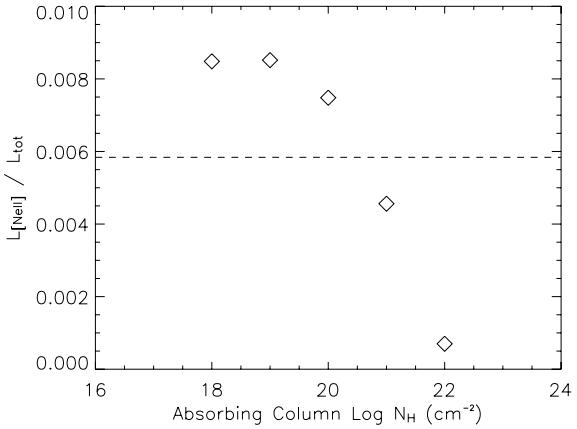

Figure 3. L([Ne II])/L_{tot} as a function of the screening column of the irradiating spectrum. The dashed line indicates the value for the unscreened spectrum.

Fig. 3 shows L([Ne II])/L_{tot} as a function of the screening column. The dashed line indicates the value predicted in the case of unabsorbed source. From this figure and from the values in Table 1, it appears that EUV radiation is less efficient at producing [Ne II] than the (soft) X-rays. In fact, even if the unscreened models have a total ionizing luminosity (X-rays+EUV) which is double than the X-ray-only luminosity, they only produce a moderate increase in L([Ne II]). This can be easily understood when one considers that [Ne II] is most efficiently produced in the low-ionization layer (just above the molecular layer; see Glassgold et al. 2007; Glassgold et al. in preparation), where a fast charge exchange with the abundant neutral H atoms quickly transforms most doubly ionized Ne into singly ionized. The charge-exchange coefficient from singly ionized to neutral Ne is instead extremely slow, conspiring to produce high abundance of Ne^+ in this warm layer. Instead, EUV radiation (>21.6 and <100 eV) can only produce Ne^+ by standard ionization of neutral Ne and is only efficient in the lower density upper atmosphere where an H II-region-like layer is formed. However, some of the Ne^+ produced in this region will be ionized to Ne^{2+} and the lower neutral H fractions in this region will result in a much less efficient charge exchange process. A spatial map of the [Ne II] emission for the unscreened model is shown in Fig. 2.

Furthermore, the models shown in Table 1 also suggest that the hard X-ray region is inefficient at the production of [Ne II] compared with the soft X-ray region. Indeed models irradiated by hard spectra with $N_H \geq 10^{21}$ cm^2 show a steep decline in the [Ne II] luminosity, even after forcing the X-ray luminosity (0.1–10 keV) to stay constant. This effect is dominated by the fact that models illuminated by a harder X-ray spectrum result to be colder (see discussion in Ercolano et al. 2009), the hard X-ray penetrate a region that is denser and cooler and therefore the resulting [Ne II] flux is reduced. Cooler models also result in flatter discs which subtend a smaller solid angle to the source of radiation.

The hardness of the spectrum has a noticeable effect on the [Ne III] 15.5 μm/[Ne II] 12.8 μm ratio. This ratio is higher for softer spectra due to the fact that doubly ionized Ne in these models can be produced in the upper layers of the disc where the neutral hydrogen fraction is lower and therefore charge exchange less efficient. Observations of the [Ne III] 15.5 μm (from now on [Ne III]) line are still rather sparse although so far low values of the [Ne III]/[Ne II] ratio have been inferred (e.g. 0.06; Lahuis et al. 2007), indicating that according to our models, at least for the few objects in question, a soft (EUV-rich) irradiating spectrum is not expected.

Our results show that changes in the irradiating spectrum can give an order of magnitude scatter (an extra factor of ∼2 is introduced when one considers that an unscreened source may contribute comparable ionizing luminosity in the EUV band that would not be accounted for in the typical L([Ne II]) versus L_X relation).

Fig. 4 (left-hand panel) shows the surface-integrated emission for some of the models discussed in this section. We find that in all cases half of the total [Ne II] emission comes from the inner regions of the

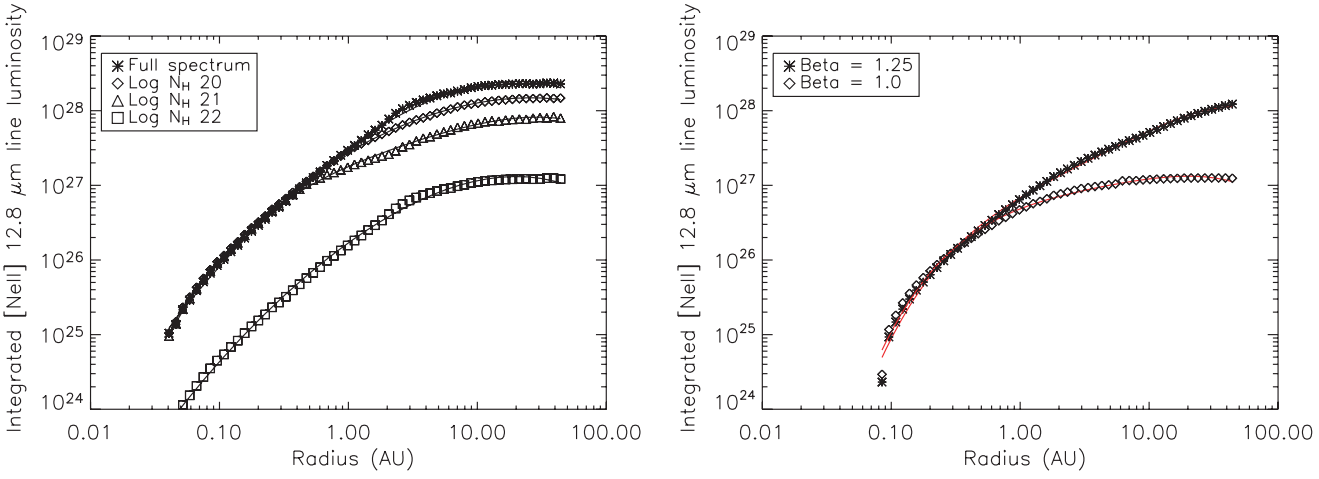

Figure 4. [Ne II] cumulative surface emission in erg s^{-1} (see the text for details). Left-hand panel: hydrostatic equilibrium models irradiated by spectra screened by various neutral hydrogen columns. Right-hand panel: flat and flared disc models computed assuming Robitaille et al. (2006) density distribution.

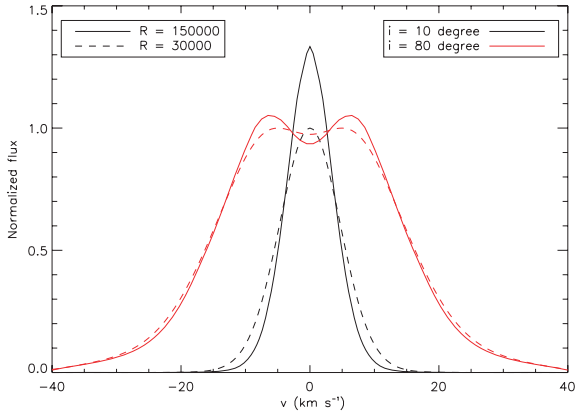

Figure 5. [Ne II] line profiles of a Keplerian disc in hydrostatic equilibrium irradiated by an unscreened EUV+X-ray source. The black lines are for low inclination ($i = 10°$) and the red lines for high inclination ($i = 80°$) discs. The solid lines have a resolution of $R = 150\,000$ and the dashed are the profiles degraded to a resolution of 30 000. For clarity the lines are normalized to the peak value of the degraded case.

disc, $\lesssim$3–4 au, so that the different spectra do not significantly affect the emission region for this line. Table 3 lists the half-luminosity and 90 per cent luminosity radii for models of various screens. As the extent of the emission region does not significantly vary with spectral hardness, the line profiles obtained are also roughly invariant. As an example, in Fig. 5 we show the [Ne II] profile for the unscreened model seen almost face on (10° inclination) and almost edge on (80° inclination), which have FWHM of ∼6–8 and ∼25–31 km s^{-1}, respectively.

Table 2. [Ne II] line luminosities computed at a range of L_X.

Model	[Ne II] (10^{28} erg s^{-1})		
$L_X(2\,10^{30}$ erg s$^{-1})$	0.1	1.0	10
Unscreened ($L_{tot} = 2L_X$)	2.9×10^{-1}	2.3	22.0
Log(N_H) = 21 ($L_{tot} = L_X$)	3.0×10^{-2}	9.1×10^{-1}	5.8
Flared ($L_{tot} = 2L_X$)	1.0×10^{-1}	1.6	17.3
Flat ($L_{tot} = 2L_X$)	1.7×10^{-2}	1.3×10^{-1}	7.0×10^{-1}

Note. The corresponding values of L_{tot} are also given.

3.2 Disc flaring

Table 2 also shows the results for the L([Ne II]) for models with flared ($\beta = 1.25$) and flat ($\beta = 1.0$) discs. A casual inspection of this table reveals roughly an order of magnitude increase in the relative luminosity of the [Ne II] line when the flaring is changed from $\beta = 1.0$ to 1.25. This is easily understood when considering that a more flared disc would subtend a larger solid angle to the irradiation source.

Disc flaring has also a dramatic effect on the size of the [Ne II] emitting region. Fig. 6 shows two-dimensional plots of the [Ne II] emissivity for the flared and flat disc models, while the right-hand panel of Fig. 4 shows the surface-integrated emission for the line for the two disc models. As summarized in Table 3, the emission region in the flared disc model extends out to a radius of ∼30 au, within which 90 per cent of the total [Ne II] luminosity is emitted. This radius is reduced to ∼6 au for the flat disc model. Naturally, this has consequences on the line profiles for these two cases, which are shown in Fig. 7 for two disc inclinations. The FWHM for the [Ne II] line produced by a flat disc seen almost edge on (inclination 80°) is roughly 40 km s^{-1}, while it is only 17 km s^{-1} for a flared disc where the emission region extends to larger cylindrical radii. The difference is of course smaller if the discs are seen almost face on (inclination 10°), thus dominated by the contribution of the thermal broadening, where a FWHM of ∼10 km s^{-1} is expected for a flat disc compared to a FWHM of ∼7 km s^{-1} for a flared disc. These statistics are summarized in Table 4.

4 DISCUSSION

As the sample of observed L([Ne II]) luminosities from protoplanetary discs continues to grow, together with the sample of pre-main-sequence stars with measured X-ray luminosities, a trend between the two quantities becomes more and more evident (Güdel et al., in preparation). While this lends evidence to the [Ne II] line being a product of X-ray irradiation of discs as predicted by Glassgold et al. (2007), the large scatter associated with this relation makes the situation less clear-cut. For a handful of objects with known powerful outflows it is clear that this line cannot be used as a diagnostics of the gaseous *disc* phase, as the emissivities may be dominated by gas in the outflows. However, even after removing objects with known

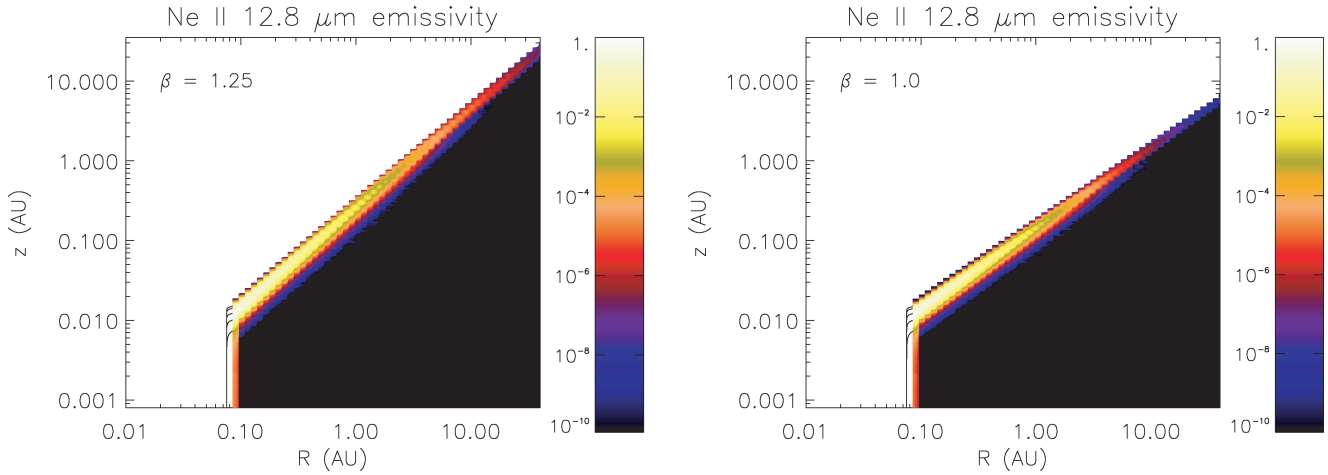

Figure 6. Two-dimensional distribution of the [Ne II] emissivity in arbitrary units. The left-hand panel refers to the disc model with $\beta = 1.25$ (flared disc), instead the right-hand panel shows the disc model with $\beta = 1.0$ (flat disc).

Table 3. Emissivity distribution statistics.

Model	Half-L radius (au)	90 per cent L radius (au)
Unscreened	2.9	10.1
Log N_h= 20	3.3	13.0
Log N_h= 21	3.5	12.8
Log N_h= 22	2.9	10.1
Flared $\beta = 1.25$	12.9	34.3
Flat $\beta = 1.0$	1.5	6.1

Note. See the text for details.

outflows from our sample we are left with approximately *one order of magnitude variations in L*([Ne II]) *at any given* L_X.

In this paper, we have investigated the origin of the large scatter observed in the [Ne II]–L_X relation. We find that variations in the irradiating spectral shape and disc structure (flaring) are sufficient to explain the typically observed scatter of approximately one order of magnitude. Fig. 8 shows the results from our models (coloured symbols) overplotted on a shaded region representing roughly the observations presented by Güdel et al. (in preparation), excluding the strong outflow objects (blue points in their plot). The definition of such region is affected by the limited sample statistic that does not allow a sharper outline, but it shows where the bulk of data falls. Moreover, we note here that we use luminosities *after* the screen while Güdel et al. use intrinsic luminosities derived from the observations. We have performed absorption calculations for a subset of the observations from which we found the following: absorbing the intrinsic X-ray spectral models by $N_H = 3 \times 10^{20}$cm^{-2}–4.6×10^{22} cm^{-2} (a range occupied by the observations) reduces the 0.1–10 keV luminosity by factors of approximately 1.4–5.5 (also depending on the intrinsic thermal model from the individual fits). On average, thus, the *unabsorbed* L_X from the observations should be shifted by a factor of 3 (0.5 dex) to the left to obtain average absorbed values, with individual shifts ranging from 0.15 to 0.75 dex. These corrections do not change the plot qualitatively. We, however, refrain from using the individual *absorbed* (post-screen) luminosities derived from the observations here because it is not clear a priori that the absorbed luminosity seen from Earth is close to the absorbed luminosity seen by the disc. The latter luminosity is principally unknown. We also mention that Güdel et al. use the 0.3–10 keV range for their luminosities, while we use 0.1–10 keV. For the post-screen luminosities for stars with $N_H > 10^{20}$ cm^{-2}, however, the difference is minor.

Our model predictions seem to agree well with the observations in terms of reproducing the scatter, and at intermediate and high X-ray luminosities the absolute values of L([Ne II]) also roughly agree with the observations. Models with low X-ray luminosities, however, fall short of the observed values, and while detection limits can partially affect the observations, the failure of our models to produce $L([\text{Ne II}]) > 10^{28}$ erg s^{-1} for X-ray luminosities of 2×10^{29} erg s^{-1} must have another origin. Nevertheless there is an overlap between our prediction for the unabsorbed source and/or the flared disc and the shaded region. Keep in mind, however, that the correction for absorption mentioned above aggravates the discrepancy between the model predictions and the observations (the latter being moved somewhat to the left in Fig. 8), but do not have effects on the conclusions on the scatter of [Ne II] luminosities.

It would be of little use here to speculate what other observational effects may be coming into play, however one thing that is worth noticing is that the measurements plotted in the figure all come from the *Spitzer Space Telescope*, while recent observations from the ground at higher resolution suggest often lower luminosities than the *Spitzer* data (Herczeg et al. 2007; Najita et al. 2009). This has been interpreted as possible pollution from molecular emission in the *Spitzer* band, while more recent works (Najita et al. 2009) seem to lean towards extended emission, from undetected outflows, which would contribute to the flux in the *Spitzer* aperture, but would be excluded by the narrow slits used for measurements from the ground.

Our results thus support a disc origin of the observed [Ne II] emission as a consequence of X-ray irradiation, at least for systems with moderate [Ne II] luminosities and absence of jets. On the other hand, the additional parameters (X-ray spectral hardness, disc flaring) now found to influence the [Ne II] luminosity add complexity to the interpretation, and the usefulness of the [Ne II] line as a disc diagnostic depends on our ability to confine these other parameters as well. Clearly, [Ne II] *disc* diagnostics needs to avoid stars with known jets and outflows. Under the assumption of full dust and gas mixing, some information about disc flaring can be obtained by modelling the infrared SED (Chiang et al. 2001; Pascucci et al. 2003), providing some important constraints on the range of modelled [Ne II] luminosities. Constraining the shape of the ionizing spectrum is perhaps the most difficult task. The intrinsic spectrum can usually be modelled sufficiently well based on

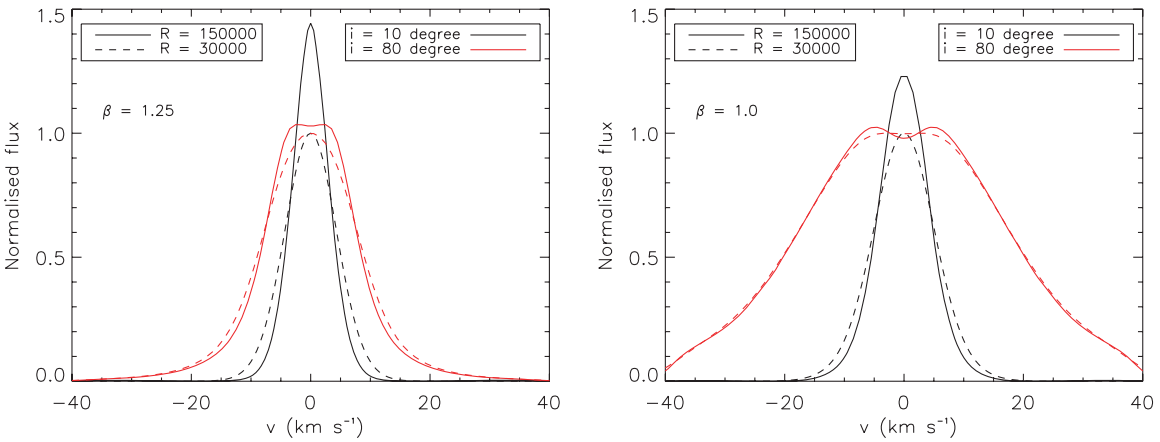

Figure 7. As in Fig. 6, but for the flared disc model ($\beta = 1.25$) (left-hand panel) and flat disc model ($\beta = 1.00$) (right-hand panel) irradiated by an unscreened EUV+X-ray spectrum.

Table 4. FWHM of the line profiles simulated for discs in Keplerian rotation viewed almost face on (10° inclination) and almost edge on (80° inclination) at two different spectral resolutions.

	Inclination 10° FWHM (km s^{-1})		Inclination 80° FWHM (km s^{-1})	
$R =$	150 000	30 000	150 000	30 000
Unscreened	8.2	11.1	31.3	32.6
Log $N_H = 21$	6.2	10.0	25.8	28.1
Flared $\beta = 1.25$	6.9	10.2	16.8	17.6
Flat $\beta = 1.0$	9.5	12.1	40.1	40.8

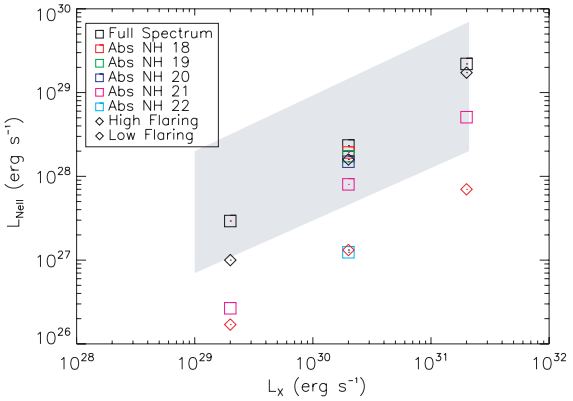

Figure 8. Comparison between the prevision of our models, where a relationship between the L([Ne II]) and L_X is expected, and the observed system with undetected outflows (from Güdel et al., in preparation).

intermediate- or high-resolution X-ray spectroscopy, but the absorbing gas column density towards the disc may be different from that towards the observer. However, in systems with weak or absent accretion or with the possible presence of inner holes, gas absorption matters the least due to the likely absence of strong winds emanating from the innermost disc regions. The [Ne II] *disc* diagnostic may thus be optimized for the study of transitional discs, most of which are also not known to drive outflows or jets. Several of these have been well studied, including new ground-based observations of spectrally resolved [Ne II] lines (Najita et al. 2009). In this context, the [Ne II] line may develop its full diagnostic power to study disc ionization and heating by ionizing radiation from the central star, processes that are pivotal for disc dispersal through photoevaporation (Alexander, Clarke & Pringle 2006; Ercolano et al. 2008a; Ercolano 2009; Owen et al., in preparation) in the first place.

High resolution and high signal-to-noise ratio line profile can help assessing the origin of the line, with profiles centred at the stellar radial velocity being synonymous with a disc origin. This is true for all inclinations except those very close to edge on, where outflows would also produce profiles centred on the stellar radial velocity. Blue shifted profiles are expected to be observed for system with outflows observed at non-edge-on inclinations (e.g. Alexander 2008), and have been recently observed by Pascucci & Sterzik (2009) in the spectra of TW Hya, Sz 73, T Cha and CS Cha. Other examples of high-resolution spectra where the line has been detected include TW Hya (Herczeg et al. 2007; $\lambda/\Delta\lambda \sim 30\,000$), GM Aur and AA Tau (Najita et al. 2009; $\lambda/\Delta\lambda \sim 80\,000$). Here the observed lines are consistent with being centred at the stellar radial velocity, suggesting a circumstellar disc origin, although the poor signal-to-noise ratio of some of these detections makes it hard to say with certainty. The lines are broad with a FWHM of respectively ∼21 (TW Hya), 70 (AA Tau) and 14 (GM Aur) km s^{-1}. The [Ne II] FWHM of GM Aur can be produced by a disc of normal flaring power; however, the large FWHM of AA Tau requires the emission region to be dominated by very small radii and therefore implies a small degree of flaring. We finally conclude that high-resolution observations of the [Ne II] line in young stellar objects, able to resolve its profile, are needed if this line is to be used to extract useful information on disc structure (flaring) and evolutionary stage by the detection of outflows and photoevaporative winds by comparison with line-profile models like those of Alexander (2008) or those presented in this work.

ACKNOWLEDGMENTS

We thank Juan Alcalá, Elvira Covino, Al Glassgold and Joan Najita for the useful comments. We further thank Thomas Robitaille for the information on the density structure of his disc model, and an anonymous referee for their useful comments. This research was supported financially from INAF (PRIN 2007: *From active accretion to debris discs*).

REFERENCES

Alexander R. D., 2008, MNRAS, 391, L64
Alexander R. D., Clarke C. J., Pringle J. E., 2004, MNRAS, 354, 71
Alexander R. D., Clarke C. J., Pringle J. E., 2006, MNRAS, 369, 229
Carr J. S., Najita J., 2008, Sci, 319, 5869, 504
Chiang E. I., Joung M. K., Creech-Eakman M. J., Qi C., Kessler J. E., Blake G. A., van Dishoeck E. F., 2001, ApJ, 547, 1077
d'Alessio P., Cantó J., Calvet N., Lizano S., 1998, ApJ, 500, 411
Dullemond C. P., Hollenback D., Kamp I., d'Alessio P., 2007, in Reipurth B., Jewitt D., Keil K., eds, Protostars & Planets V. Univ. Arizona Press, Tucson, p. 555
Ercolano B., Storey P. J., 2006, MNRAS, 372, 1875
Ercolano B., Barlow M. J., Storey P. J., Liu X.-W., 2003, MNRAS, 340, 1136
Ercolano B., Barlow M. J., Storey P. J., 2005, MNRAS, 362, 1038
Ercolano B., Drake J. J., Raymond J. C., Clarke C. J., 2008a, ApJ, 688, 398
Ercolano B., Young P. R., Drake J. J., Raymond J. C., 2008b, ApJSS, 175, 534
Ercolano B., Clarke C. J., Drake J. J., 2009, ApJ, 699, 1639
Espaillat C., Calvet N., D'Alessio P., Bergin E., 2007, ApJ, 664, L111
Glassgold A. E., Najita J. R., Igea J., 2007, ApJ, 656, 515
Gorti U., Hollenback D., 2008, ApJ, 615, 972
Grevesse N., Sauval A. J., 1998, Space Sci. Rev., 85, 161
Güdel M. et al., 2007, A&A, 468, 529
Güdel M., Skinner S. L., Audard M., Briggs K. R., Cabrit S., 2008, A&A, 478, 797
Hayashi C., 1981, Progress of Theoretical Physics Supplement, No. 70, p. 35
Herczeg G. J., Linsky J. L., Valenti J. A., Johns-Krull C. M., Wood B. E., 2002, ApJ, 572, 310
Herczeg G. J., Najita J. R., Hillenbrand L. A., Pascucci I., 2007, ApJ, 670, 509
Hollenbach D., Gorti U., 2009, ApJ, 703, 1203
Kashyap V., Drake J. J., 2000, Bull. Astron. Soc. India, 28, 475
Kuchner M. J., 2004, ApJ, 612, 1147
Lahuis F., van Dishoeck E. F., Blake G. A., Evans N. J. et al., 2007, ApJ, 665, 492
Landi E., Phillips K. J. H., 2006, ApJS, 166, 421
Mazzotta P., Mazzitelli G., Colafrancesco S., Vittorio N., 1998, A&AS, 133, 403
Meijerink R., Glassgold A. E., Najita J. R., 2008, ApJ, 676, 518

Najita J. R., Carr J. S., Glassgold A. E., Valenti J., 2007, in Reipurth B., Jewitt D., Keil K., eds, Protostars & Planets V. Univ. Arizona Press, Tucson, p. 507
Najita J. R. et al., 2009, ApJ, 697, 957
Natta A., Testi L., Calvet N., Henning Th., Waters R., Wilner D., 2007, in Reipurth B., Jewitt D., Keil K., eds, Protostars & Planets V. Univ. Arizona Press, Tucson, p. 555
Owen J., Ercolano B., Clarke C. J., Alexander R. D., 2009, MNRAS, submitted
Pascucci I., Sterzik M., 2009, ApJ, 702, 724
Pascucci I., Apai D., Henning Th., Dullemond C. P., 2003, ApJ, 590, L111
Pascucci I. et al., 2007, ApJ, 663, 383
Robitaille T. P., Whitney B. A., Indebetouw R., Wood K., Denzmore P., 2006, ApJS, 167, 256
Salyk C. et al., 2008, ApJ, 676, L49
van Boekel R., Güdel M., Henning Th., Lahuis F., Pantin E., 2009, A&A, 497, 137
Verner D. A., Yakovlev D. G., Band L. M., Trzhaskovskaya M. B., 1993, Atomic Data Nucl. Data Tables, 55, 233
Verner E. M., Yakovlev D. G., 1995, A&AS, 109, 125
Weingartner B. C., Draine B. T., 2001, ApJ, 548, 296
Whitney B. A., Wood K., Bjorkman J. E., Wolff M. J., 2003a, ApJ, 591, 1049
Whitney B. A., Wood K., Bjorkman J. E., Cohen M., 2003b, ApJ, 598, 1079

This paper has been typeset from a TEX/LATEX file prepared by the author.